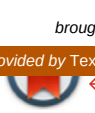

Assessing the effects of anthropogenic aerosols on Pacific storm track using a multiscale global climate model

Yuan Wang[a,b], Minghuai Wang[c], Renyi Zhang[a,d,1], Steven J. Ghan[c], Yun Lin[a], Jiaxi Hu[a], Bowen Pan[a], Misti Levy[a], Jonathan H. Jiang[b], and Mario J. Molina[e,1]

[a]Department of Atmospheric Sciences, Texas A&M University, College Station, TX 77843; [b]Jet Propulsion Laboratory, California Institute of Technology, Pasadena, CA 91109; [c]Pacific Northwest National Laboratory, Richland, WA 99354; [d]State Key Joint Laboratory of Environmental Simulation and Pollution Control, College of Environmental Sciences and Engineering, Peking University, Beijing 100871, China; and [e]Department of Chemistry and Biochemistry, University of California, San Diego, La Jolla, CA 92093

Contributed by Mario J. Molina, March 11, 2014 (sent for review December 28, 2013; reviewed by Zhanqing Li and Yangang Liu)

Atmospheric aerosols affect weather and global general circulation by modifying cloud and precipitation processes, but the magnitude of cloud adjustment by aerosols remains poorly quantified and represents the largest uncertainty in estimated forcing of climate change. Here we assess the effects of anthropogenic aerosols on the Pacific storm track, using a multiscale global aerosol–climate model (GCM). Simulations of two aerosol scenarios corresponding to the present day and preindustrial conditions reveal long-range transport of anthropogenic aerosols across the north Pacific and large resulting changes in the aerosol optical depth, cloud droplet number concentration, and cloud and ice water paths. Shortwave and longwave cloud radiative forcing at the top of atmosphere are changed by −2.5 and +1.3 W m^{-2}, respectively, by emission changes from preindustrial to present day, and an increased cloud top height indicates invigorated midlatitude cyclones. The overall increased precipitation and poleward heat transport reflect intensification of the Pacific storm track by anthropogenic aerosols. Hence, this work provides, for the first time to the authors' knowledge, a global perspective of the effects of Asian pollution outflows from GCMs. Furthermore, our results suggest that the multiscale modeling framework is essential in producing the aerosol invigoration effect of deep convective clouds on a global scale.

aerosol-cloud–climate interaction | convective storms, cloud invigoration

Atmospheric aerosols, formed from both natural and anthropogenic sources (1, 2), affect the Earth's energy budget directly, by scattering or absorbing solar radiation, and indirectly, by altering cloud microphysical characteristics and regulating the hydrological cycle (3–5). In particular, the aerosols have an indirect effect by serving as cloud condensation nuclei, and their interaction with the microphysics and dynamics of deep convective clouds (DCCs) may modify the cloud structure and redistribute latent heating (6), leading to an enhanced precipitation efficiency (7–12), invigorated convection strength (13–15), and intensified lightning activities (16–18). At this time, the indirect radiative forcing of anthropogenic aerosols represents the least-understood component in the forcing of climate change (19, 20).

Increasing levels of particulate matter (PM) pollutants from the Asian continent and their associated outflows have raised considerable concern because of their potential effects on regional climate and global atmospheric circulation (21–23). Intense emissions of anthropogenic aerosols and their long-range transport from Asia are clearly documented by satellite and in situ measurements (21, 22). Zhang and colleagues (23) first suggested that Asian pollution likely accounts for a climatically increased DCC amount over the north Pacific on the basis of long-term analysis of cloud measurements from the International Satellite Cloud Climatology Project and high-resolution infrared sounder. In addition, a trend of increasing wintertime precipitation over the north Pacific has been identified from Global Precipitation Climatology Project measurements (24). The effects of anthropogenic aerosols on DCC systems over the north Pacific have been modeled in episodic simulations, using a regional cloud-resolving model (CRM) with a two-moment bulk microphysical scheme (23, 24). Most recently, on the basis of hierarchical modeling and observational analysis, it has been suggested that midlatitude cyclones are modulated by Asian pollution (25).

At this time, an explicit representation of cloud microphysical processes in global climate models (GCM) is computationally impractical. Because the vertical velocity and latent heating within DCCs are crudely diagnosed in traditional convective cloud parameterizations, the pathway of aerosols in affecting clouds and the precipitation of DCCs is not properly accounted for in GCMs, and most of those models are incapable of investigating the complicated interaction between aerosols and DCCs. To overcome such inherent deficiencies of GCMs, a multiscale modeling framework (MMF) has been developed (26). The first MMF model was built at the Colorado State University, replacing the cloud parameterizations in a host Community Atmospheric Model (CAM) with a 2D version of the cloud-resolving System for Atmospheric Modeling embedded within each grid column of CAM to resolve subgrid variability in

Significance

Increasing levels of air pollutants in Asia have recently drawn considerable attention, but the effects of Asian pollution outflows on regional climate and global atmospheric circulation remain to be quantified. Using a multiscale global aerosol–climate model (GCM), we demonstrate long-range transport of the Asian pollution, large resulting variations in the aerosol optical depth, cloud droplet number concentration, and cloud and ice water paths; enhanced shortwave and longwave cloud radiative forcings; and increased precipitation and poleward heat transport. Our work provides, for the first time to the authors' knowledge, a global multiscale perspective of the climatic effects of pollution outflows from Asia. The results reveal that the multiscale modeling framework is essential in simulating the aerosol invigoration effect of deep convective cloud systems by a GCM.

Author contributions: Y.W., M.W., R.Z., and M.J.M. designed research; Y.W., M.W., and R.Z. performed research; Y.W., M.W., R.Z., S.J.G., Y.L., J.H., B.P., M.L., J.H.J., and M.J.M. analyzed data; and Y.W. and R.Z. wrote the paper.

Reviewers: Z.L., University of Maryland; Y.L., Brookhaven National Laboratory.

The authors declare no conflict of interest.

[1]To whom correspondence may be addressed. E-mail: renyi-zhang@tamu.edu or mjmolina@ucsd.edu.

This article contains supporting information online at www.pnas.org/lookup/suppl/doi:10.1073/pnas.1403364111/-/DCSupplemental.

the dynamics and microphysics of clouds. As an extension to the Colorado State University MMF, an aerosol version has been developed at the Pacific Northwest National Laboratory (PNNL-MMF), using an explicit-cloud parameterized-pollutant approach to link the cloud processing of aerosols on the large-scale grid with the cloud/precipitation statistics in the System for Atmospheric Modeling and replacing the one-moment cloud microphysics scheme in the System for Atmospheric Modeling with a two-moment scheme to permit simulation of the interactions between aerosols and hydrometeors (27, 28).

In this article, we investigate the transport process of anthropogenic aerosols over the north Pacific and the resulting effects on the Pacific storm track, using the results of explicitly simulated chemical, aerosol, and cloud processes for both convective and stratiform clouds on a global scale from the PNNL-MMF. Two aerosol scenarios, corresponding to 2000 and 1850, were chosen to represent present-day (PD) and preindustrial (PI) emissions, respectively, based on emissions from the Intergovernmental Panel on Climate Change Fifth Assessment Report (19, 20).

Results and Discussion

Anthropogenic emissions from Asia produce significant increases in aerosol optical depth (AOD) over the northwest Pacific (Fig. 1*A*), with the largest increases near sources on the Asian continent. The zonal extension of enhanced AOD reflects the transport of PM pollution from East Asia to the Pacific (Fig. S1). AOD is increased by 0.03 in the PD case, averaged over the northwest Pacific, which is a 46% relative increase. Most of the increase in the aerosol mass concentration over the northwest Pacific (Fig. 1*B*) is a result of anthropogenic sulfate, which increases sulfate concentration more than threefold. In addition, the concentrations of primary organic carbon and black carbon (BC) also increase by 3–5 times in PD compared with PI. The ratio of sulfate to the total aerosol mass concentrations increases from 30% to 53%. In contrast, the aerosol concentrations from natural sources, such as dust and sea salt, are relatively unchanged in the two aerosol scenarios. Clearly, the enhanced AOD over the northwest Pacific in the PD scenario confirms efficient transport of anthropogenic aerosols from the Asian continent and is consistent with previous satellite and in situ aerosol measurements in this region (21–23).

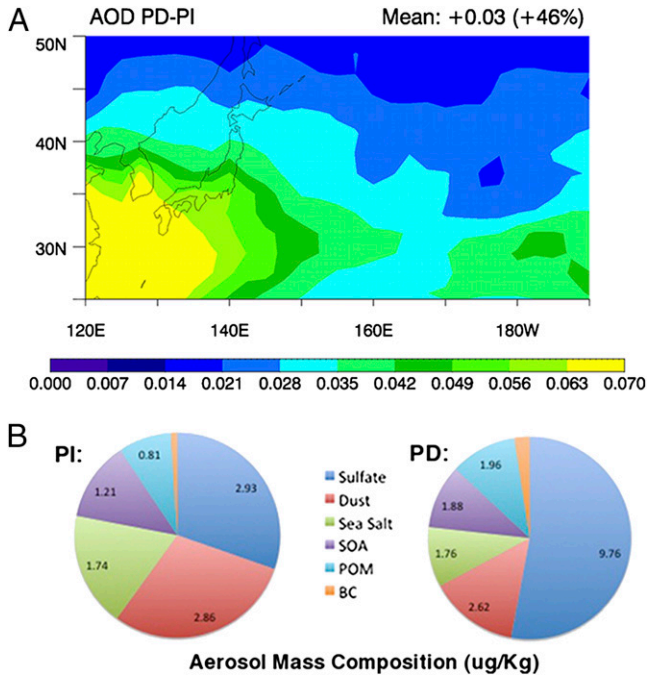

Fig. 1. Aerosol properties over the northwest Pacific from PNNL-MMF. (*A*) The difference of AOD between PD and PI. (*B*) The comparison of aerosol mass concentration and chemical composition in the accumulation mode between PD and PI.

The coupling between convective clouds and Asian pollution outflows produces significant effects on cloud properties, atmospheric radiative forcing, and poleward heat transport (Fig. 2). The increased sulfate aerosol concentration in PD increases the cloud droplet number concentration substantially over the northwest Pacific (Fig. 2*A*), with the largest increase near the pollution sources and an average relative increase of 108%. The total liquid water path (LWP) is enhanced by 5.6 g m^{-2} (9.8%) compared with the PI case (Fig. 2*B*), indicating the delay of warm precipitation in the presence of the larger number of small cloud droplets with the PM pollution outflows.

Because the enhancement ratio of the liquid water content (9.8%) is much less than that of cloud number concentration (108%) in PD, the cloud effective radius is reduced by 13% in the PD scenario. The average ice water path (IWP) increases by 0.7 g m^{-2} (9%) over the northwest Pacific in the PD case (Fig. 2*C*), suggesting more efficient mixed-phase processes, such as droplet freezing and riming of ice crystals above the freezing level. As a consequence, the anvil of convective clouds is broadened over the storm track. The enhanced IWP is located in the center of the north Pacific region (around 180° E) downstream of the storm track, downwind from the location of enhanced LWP, close to the Asian continent. Examination of the spatial distributions of LWP and IWP in PD and PI (Figs. S2 and S3) reveals that liquid-phase water dominates in clouds over the west Pacific, but ice clouds become abundant in the middle of the ocean. The geospatial difference between the LWP and IWP enhancement over the northwest Pacific suggests that anthropogenic aerosols have an effect on the various cloud types throughout the life cycle of cyclones. The major enhancement of the high cloud fraction (Fig. 2*D*) is located downstream of the storm track, coinciding with elevated IWP in the center of the north Pacific. The 2.6% relative increase in the high cloud fraction averaged over the northwest Pacific is consistent with the observed climatologic trend of increasing high clouds on the basis of the International Satellite Cloud Climatology Project and high-resolution infrared sounder satellite cloud measurements (23).

The changes in LWP, IWP, and droplet effective radius produce changes in cloud radiative forcing at the top of atmosphere (TOA). The shortwave cloud radiative forcing at TOA (Fig. 2*E*) over the northwest Pacific becomes stronger by 2.5 W m^{-2} because of a reduced cloud particle effective size and enhanced LWP in the PD case, both producing stronger cooling. The longwave cloud radiative forcing at TOA is increased by 1.3 W m^{-2} in the PD case (Fig. 2*F*), providing stronger atmospheric warming, especially at nighttime. Because the spatial pattern of longwave cloud radiative forcing enhancement is consistent with that of IWP and high cloud frequency, a greater amount of high-level ice clouds is likely responsible for the reduced outgoing longwave radiation at TOA in the PD scenario. The warming effects on longwave radiation from the enlarged anvils of convective clouds induced by aerosols are consistent with previous studies from satellite measurements (29) and CRM simulations (30).

Although aerosol direct effects on atmospheric radiation fluxes are explicitly represented in PNNL-MMF, the influence of aerosol scattering on the shortwave radiation budget is limited because of the large cloud fraction over the wintertime Pacific, and absorption by BC is effective only if the BC is above clouds. The aerosol effect on the clear-sky shortwave downward flux at the surface over the northwest Pacific is −2.5 W m^{-2}, which is

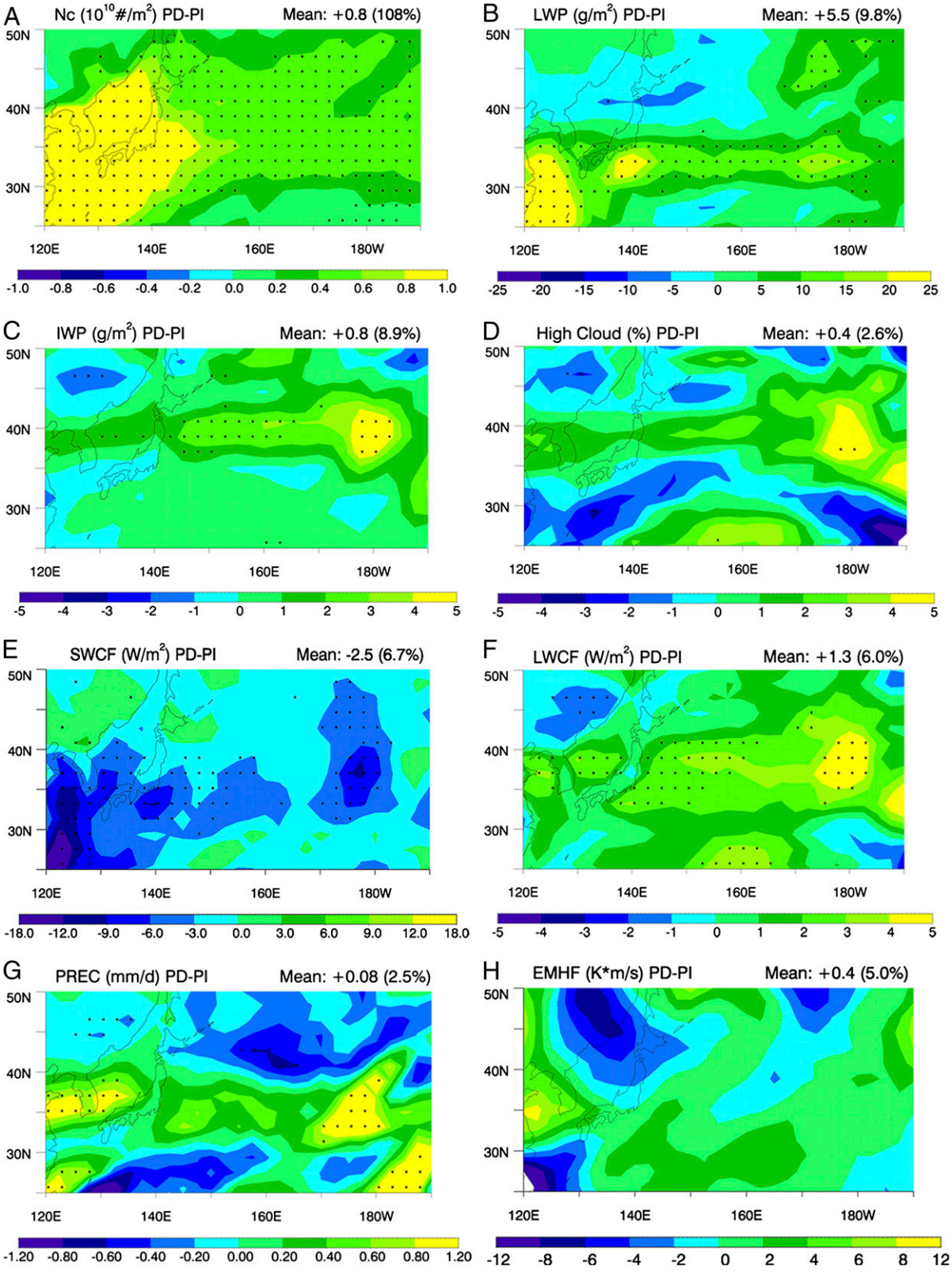

Fig. 2. The differences in cloud, radiative, and EMHF between PD and PI over the northwest Pacific from PNNL-MMF. (*A*) Cloud number concentration, (*B*) LWP, (*C*) IWP, (*D*) high cloud fraction, (*E*) shortwave cloud radiative forcing at TOA, (*F*) longwave cloud radiative forcing at TOA, (*G*) precipitation, and (*H*) EMHF at 850 hPa smoothed by an 8-d high pass filter. The black dots indicate regions with *t* test significance of larger than 90%.

much less than the all-sky effect of −5.0 W m^{-2}, because the aerosol indirect effect dominates (Fig. S4).

The response of precipitation to the different aerosol scenarios is nonuniform over the northwest Pacific (Fig. 2*G*). For the rainfall bell characteristic of the Pacific storm track (Fig. S5), enhanced precipitation mainly occurs in areas with a heavy mean precipitation rate (>6 mm d^{-1}). The precipitation rate averaged over the northwest Pacific is increased by about 2.4%, consistent with an observed decadal trend of increasing precipitation over this region (24).

The Pacific storm track represents a critical component in the global general circulation by transporting heat and moisture fluxes. The simulated transient eddy meridional heat flux (EMHF) at 850 hPa over the northwest Pacific (Fig. 2*H*) increases by 5% in the PD scenario. The increase is more pronounced over the storm track downstream, indicating that the heat transport associated with the Pacific storm track is intensified under the influence of the Asian pollution outflow. The enhancement of EMHF over the northwest Pacific by anthropogenic aerosols is in agreement with predictions using hierarchical modeling and from reanalysis data (25).

The aerosol invigoration of convective storms is further evident in the vertical profiles of the convective cloud amount and cloud top height. Fig. 3 shows the PD − PI differences in the vertical profiles of the amount of convective clouds (diagnosed in the PNNL-MMF model by using CRM cloud statistics) and the cloud top fraction. The coverage of shallow convective clouds (lower than 850 hPa) is slightly larger in PD than in PI throughout the northwest Pacific, and an even larger increase of middle-level tconvective clouds (between 850 and 400 hPa) occurs in remote maritime areas to the west of 150° E (Fig. 3*A*). Greater cloud water contents and strengthened updrafts (Fig. S6) are responsible for the larger coverage of convective clouds in the PD case. Fig. 3*B* shows that the cloud top heights are considerably different between PD and PI. In the troposphere above 600 hPa, the cloud top fraction increases by 10–20%, but clouds with heights lower than 600 hPa are significantly reduced in the center of the northwest Pacific from 140° E to 170° E. The modified cloud structure and elevated cloud top height provide direct evidence of aerosol-induced invigoration of DCC development, consistent with satellite measurements over the Pacific and Atlantic regions (23, 31).

Our findings on aerosol–cloud–precipitation interactions over the northwest Pacific are consistent with those from CRM simulations (30, 32) and from long-term surface and global satellite observations (13, 33). To illustrate how essential it is to explicitly resolve the cloud updrafts in the PNNL-MMF, we compare the cloud invigoration response in the PNNL-MMF to the response in the host GCM (CAM5) when cloud parameterization (34) is used to represent deep convection, rather than embedded CRMs. CAM5 treats cloud–aerosol interactions for stratiform clouds but does not resolve convective clouds. Simulations by CAM5 are performed using the same Intergovernmental Panel on Climate Change Fifth Assessment Report emission datasets to represent PD and PI conditions. Comparison of AOD between PD and PI shows that AOD in the PD case increases by 0.02, averaged over the northwest Pacific (Fig. 4*A*), in agreement with the increase of 0.03 in AOD from PNNL-MMF. Because of an increased cloud droplet concentration and a reduced droplet effective size in CAM5, LWP is increased by 10 g m^{-2} in PD, leading to a relative increase of LWP by 33%, which is much larger than the 10% relative increase of LWP in PNNL-MMF (Fig. 4*B*). A global comparison between CAM5 and PNNL-MMF (28) also indicates that the response of LWP to a given cloud condensation nuclei perturbation in PNNL-MMF is about one-third that in CAM5. Noticeably, CAM5 predicts reduced IWP in the PD case over the northwest Pacific region, in contrast to the enhanced IWP by PNNL-MMF (Fig. 4*C*). In addition, CAM5 simulations yield a reduced convection depth in the PD case (Fig. S6), indicating that the convective strength of storms over the northwest Pacific is suppressed. In addition, a weakened cyclone intensity in the PD scenario from CAM5 simulations further leads to a 3% reduction of surface precipitation from convective clouds over the northwest Pacific (Fig. 4*D*). Thus, CAM5 without multiscale modeling yields little aerosol invigoration of convective clouds and overpredicts aerosol indirect effects on stratiform clouds. The response of LWP to increasing aerosol in PNNL-MMF has been found to be much more realistic than that in CAM5 without multiscale modeling (35).

The simulations from the PNNL-MMF multiscale aerosol–GCM clearly illustrate long-range transport of anthropogenic aerosols from Asia to the Pacific region. The results with greater anthropogenic aerosol loading yield decreased shortwave and increased longwave cloud radiative forcing at the TOA and increased precipitation and poleward heat transport. In addition, the increasing amount of high-level clouds indicates invigorated cyclones by anthropogenic aerosols. The differences in the spatial distributions of LWP and IWP changes suggest that anthropogenic aerosols likely exert distinct effect on the various cloud types throughout the lifecycle of cyclones. Hence, our results corroborate previous findings indicating that transport of Asian anthropogenic aerosols leads to an intensified Pacific storm track (23–25), providing for the first time to the authors' knowledge a global perspective of the effects of Asian pollution outflows from GCMs. Furthermore, our results suggest that

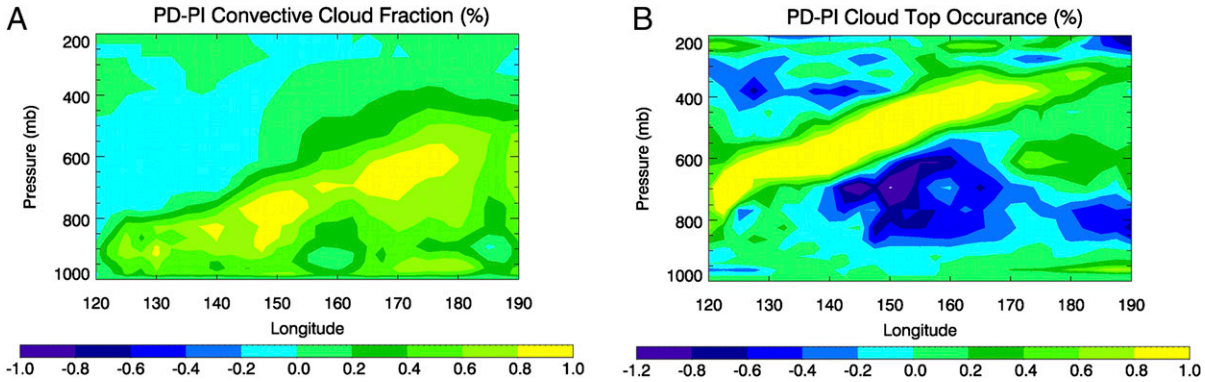

Fig. 3. The differences in the vertical distribution of (*A*) convective cloud fraction and (*B*) the frequency of the cloud top occurrence between PD and PI over the northwest Pacific from PNNL-MMF.

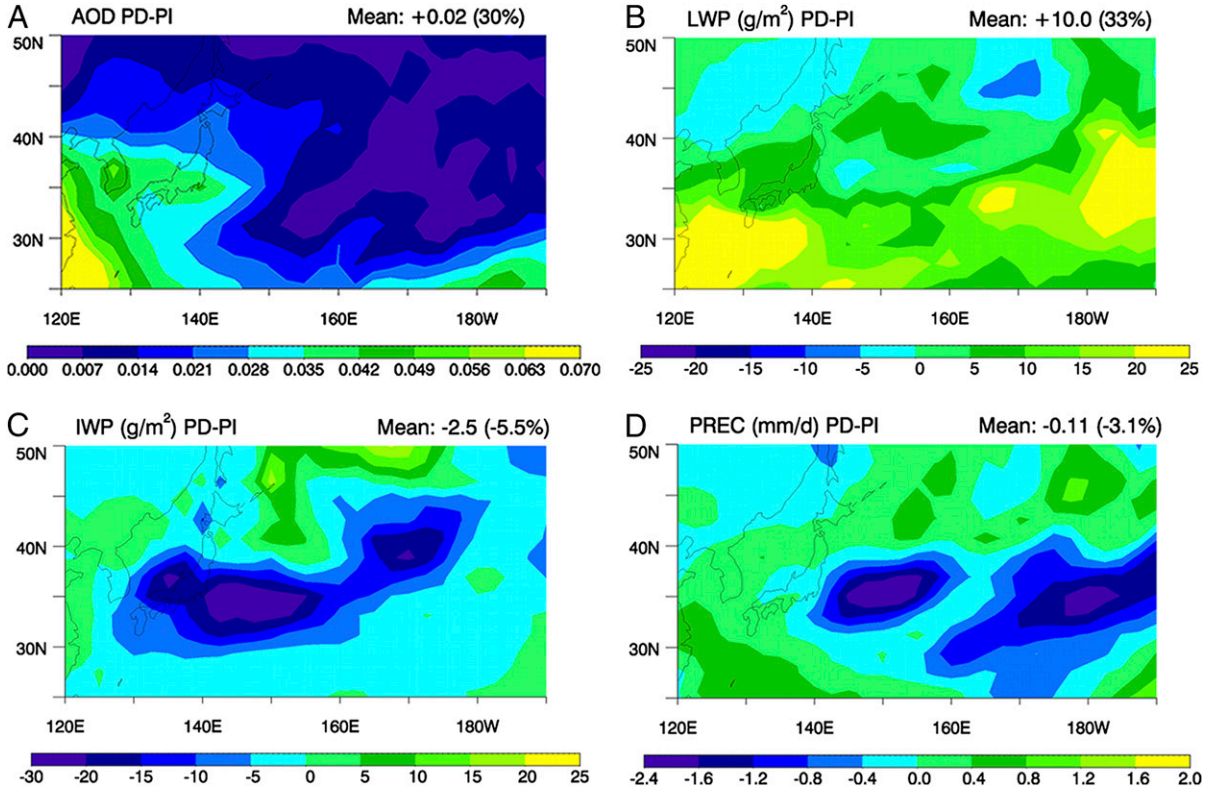

Fig. 4. The differences in (*A*) AOD, (*B*) LWP, (*C*) IWP, and (*D*) precipitation between PD and PI over the northwest Pacific from CAM5 simulations.

inclusion of the multiscale framework in GCMs is critical in producing the aerosol invigoration effect of DCCs on a global scale.

Methods

Six-year global climate simulations driven by the climatological sea surface temperature were carried out, using PNNL-MMF. Simulations with the conventional host CAM5 alone were also conducted to compare with the performance of PNNL-MMF. Both the host CAM5 and PNNL-MMF runs were performed at a 1.9° × 2.5° horizontal resolution with 30 vertical levels. The years 2000 and 1850 were chosen to represent the PD and PI cases, respectively. The global sources and burden of six types of aerosols considered in PD and PI cases, including sulfate, BC, primary organic matter, secondary organic aerosol (SOA), dust, and sea salt. Anthropogenic SO_2, BC, and primary organic matter data are taken from the Intergovernmental Panel on Climate Change Fifth Assessment Report. Emissions of other aerosol precursors and the formation mechanisms of SOA have been described previously (27, 28). SOA formation is contributed from atmospheric photochemical oxidation products of biogenic and anthropogenic hydrocarbons (36–38), although particle-phase reactions leading to SOA formation have yet to be included in atmospheric models (39, 40). Sea salt particles are assumed to contain mainly sodium chloride, although a recent study has indicated that sea spray aerosols may contain significant biological species, including bacteria, phytoplankton, and viruses (41). The northwest Pacific area (25° N–50° N, 120° E–170° W) was focused on in this study. Monthly simulations in January and February were considered, as the Pacific storm track is most active in wintertime (42) and because transport of the Asian pollution also peaks from January to March annually (43).

ACKNOWLEDGMENTS. The authors acknowledge T. Yuan and P. Liss for providing additional comments. This work was supported by a National Aeronautics and Space Administration (NASA) Graduate Student Fellowship in Earth System Science (to Y.W.), Ministry of Science and Technology of China Award (2013CB955800 to R.Z.), the NASA Research Opportunities in Space and Earth Sciences Enhancing the Capability of Computational Earth System Models and Using NASA Data for Operation and Assessment program at the Jet Propulsion Laboratory, California Institute of Technology, under contract with NASA (Y.W. and J.H.J.), and the Department of Energy (DOE) Office of Science, Decadal and Regional Climate Prediction using Earth System Models program (M.W. and S.J.G.). PNNL is operated by Battelle for the DOE under Contract DE-AC06-76RLO 1830. This research used resources of the Oak Ridge Leadership Computing Facility at the Oak Ridge National Laboratory, which is supported by the Office of Science of the US Department of Energy under Contract DE-AC05-00OR22725.

1. Zhang R, Khalizov AF, Wang L, Hu M, Xu W (2012) Nucleation and growth of nanoparticles in the atmosphere. *Chem Rev* 112(3):1957–2011.
2. Zhang R (2010) Atmospheric science. Getting to the critical nucleus of aerosol formation. *Science* 328(5984):1366–1367.
3. Lohmann U, Feichter J (2005) Global indirect aerosol effects: A review. *Atmos Chem Phys* 5:715–737.
4. Rosenfeld D, et al. (2008) Flood or drought: How do aerosols affect precipitation? *Science* 321(5894):1309–1313.
5. Tao W-K, Chen J-P, Li Z, Wang C, Zhang C (2012) Impact of aerosols on convective clouds and precipitation. *Rev Geophys* 50(2).
6. Rosenfeld D, et al. (2012) Aerosol Effects on Microstructure and Intensity of Tropical Cyclones. *Bull Am Meteorol Soc* 93(7):987–1001.
7. Khain A, Rosenfeld D, Pokrovsky A (2005) Aerosol impact on the dynamics and microphysics of deep convective clouds. *Q J R Meteorol Soc* 131(611):2639–2663.
8. Li G, Wang Y, Zhang R (2008) Implementation of a two-moment bulk microphysics scheme to the WRF model to investigate aerosol-cloud interaction. *J Geophys Res* 113:D15211.
9. Koren I, et al. (2012) Aerosol-induced intensification of rain from the tropics to the mid-latitudes. *Nat Geosci* 5(2):118–122.
10. Fan J, Zhang R, Tao W-K, Mohr K (2008) Effects of aerosol optical properties on deep convective clouds and radiative forcing. *J Geophys Res* 113:D08209.
11. Fan J, Zhang R, Li G, Tao W-K (2007) Effects of aerosols and relative humidity on cumulus clouds. *J Geophys Res* 112:D14204.
12. Li G, Wang Y, Lee K-H, Diao D, Zhang R (2009) The impacts of aerosols on development and precipitation of a mesoscale squall line. *J Geophys Res* 114: D17205.
13. Li Z, et al. (2011) Long-term impacts of aerosols on the vertical development of clouds and precipitation. *Nat Geosci* 4(12):888–894.
14. Fan J, Zhang R, Li G, Tao W-K, Li X (2007) Simulations of cumulus clouds using a spectral microphysics cloud resolving model. *J Geophys Res* 112:D04201.
15. Yuan T, Li Z, Zhang R, Fan J (2008) Increase of cloud droplet size with aerosol optical depth: An observation and modeling study. *J Geophys Res* 113:D04201.
16. Orville RE, et al. (2001) Enhancement of Cloud-to-Ground Lightning over Houston, Texas. *Geophys Res Lett* 28:2597–2600.

17. Wang Y, et al. (2011) Long-term impacts of aerosols on precipitation and lightning over the Pearl River Delta megacity area in China. *Atmos Chem Phys* 11(23):12421–12436.
18. Yuan T, Remer LA, Pickering KE, Yu H (2011) Observational evidence of aerosol enhancement of lightning activity and convective invigoration. *Geophys Res Lett* 38: L04701.
19. Stocker T, et al. (2013) Climate change 2013: The physical science basis. Intergovernmental Panel on Climate Change, Working Group I Contribution to the IPCC Fifth Assessment Report (AR5) (Cambridge Univ Press, New York).
20. Ghan SJ, et al. (2012) Toward a Minimal Representation of Aerosols in Climate Models: Comparative Decomposition of Aerosol Direct, Semidirect, and Indirect Radiative Forcing. *J Clim* 25(19):6461–6476.
21. Yu H, et al. (2008) A satellite-based assessment of transpacific transport of pollution aerosol. *J Geophys Res* 113:D14S12.
22. Mochida M, et al. (2011) Hygroscopicity and cloud condensation nucleus activity of marine aerosol particles over the western North Pacific. *J Geophys Res* 116:D06204.
23. Zhang R, Li G, Fan J, Wu DL, Molina MJ (2007) Intensification of Pacific storm track linked to Asian pollution. *Proc Natl Acad Sci USA* 104(13):5295–5299.
24. Li G, Wang Y, Lee K-H, Diao Y, Zhang R (2008) Increased winter precipitation over the North Pacific from 1984–1994 to 1995–2005 inferred from the Global Precipitation Climatology Project. *Geophys Res Lett* 35:L13821.
25. Wang Y, Zhang R, Saravanan R (2014) Asian pollution climatically modulates midlatitude cyclones following hierarchical modelling and observational analysis. *Nat Commun* 5:3098.
26. Khairoutdinov MF, Randall DA (2001) A cloud resolving model as a cloud parameterization in the NCAR Community Climate System Model: Preliminary results. *Geophys Res Lett* 28(18):3617–3620.
27. Wang M, et al. (2011) The multi-scale aerosol-climate model PNNL-MMF: Model description and evaluation. *Geosci Model Dev* 4(1):137–168.
28. Wang M, et al. (2011) Aerosol indirect effects in a multi-scale aerosol-climate model PNNL-MMF. *Atmos Chem Phys* 11(11):5431–5455.
29. Koren I, Remer LA, Altaratz O, Martins JV, Davidi A (2010) Aerosol-induced changes of convective cloud anvils produce strong climate warming. *Atmos Chem Phys* 10(10): 5001–5010.
30. Fan J, Rosenfeld D, Ding Y, Leung LR, Li Z (2012) Potential aerosol indirect effects on atmospheric circulation and radiative forcing through deep convection. *Geophys Res Lett* 39:L09806.
31. Koren I, Kaufman YJ, Rosenfeld D, Remer LA, Rudich Y (2005) Aerosol invigoration and restructuring of Atlantic convective clouds. *Geophys Res Lett* 32:L14828.
32. Wang Y, et al. (2013) Improving bulk microphysics parameterizations in simulations of aerosol effects. *J Geophys Res* 118:5361–5379.
33. Niu F, Li Z (2012) Systematic variations of cloud top temperature and precipitation rate with aerosols over the global tropics. *Atmos Chem Phys* 12:8491–8498.
34. Liu X, et al. (2012) Toward a minimal representation of aerosols in climate models: Description and evaluation in the Community Atmosphere Model CAM5. *Geosci Model Dev* 5:709–739.
35. Wang M, et al. (2012) Constraining cloud lifetime effects of aerosol using A-Train satellite observations. *Geophys Res Lett* 39:L15709.
36. Zhao J, et al. (2005) Experimental product study of the OH-initiated oxidation of m-xylene. *J Photoch Photobio A* 176:199–207.
37. Lei W, et al. (2001) Theoretical study of OH-O_2-isoprene peroxy radicals. *J Phys Chem* 105:471–477.
38. Lei W, et al. (2000) Theoretical study of isomeric branching in the isoprene-OH reaction: Implications to final product yields in isoprene oxidation. *Chem Phys Lett* 326: 109–114.
39. Wang L, Lal V, Khalizov AF, Zhang R (2010) Heterogeneous chemistry of alkylamines with sulfuric acid: Implications for atmospheric formation of alkylaminium sulfates. *Environ Sci Technol* 44(7):2461–2465.
40. Zhao J, Levitt NP, Zhang R (2005) Heterogeneous chemistry of octanal and 2, 4-hexadienal with sulfuric acid. *Geophys Res Lett* 32:L09802.
41. Prather KA, et al. (2013) Bringing the ocean into the laboratory to probe the chemical complexity of sea spray aerosol. *Proc Natl Acad Sci USA* 110(19):7550–7555.
42. Nakamura H, Izumi T, Sampe T (2002) Interannual and decadal modulations recently observed in the Pacific storm track activity and east Asian winter monsoon. *J Clim* 15(14):1855–1874.
43. Liu HY, et al. (2003) Transport pathways for Asian pollution outflow over the Pacific: Interannual and seasonal variations. *J Geophys Res* 108:D20.